Zero Temperature Phases of the Electron Gas

G. $Ortiz^a$, M. Harris^b, and P. Ballone^c

(a) Theoretical Division, Los Alamos National Laboratory, P.O. Box 1663, Los Alamos, NM 87545

(b) Max-Planck Institut für Festkörperforschung, Heisenbergstrasse 1, 70569 Stuttgart, Germany

(c) Institut für Festkörperforschung Forschungszentrum Jülich, 52425 Jülich, Germany

(November 1, 2021)

The stability of different phases of the three-dimensional non-relativistic electron gas is analyzed using stochastic methods. With decreasing density, we observe a *continuous* transition from the paramagnetic to the ferromagnetic fluid, with an intermediate stability range $(25 \pm 5 \le r_s \le 35 \pm 5)$ for the *partially* spin-polarized liquid. The freezing transition into a ferromagnetic Wigner crystal occurs at $r_s = 65 \pm 10$. We discuss the relative stability of different magnetic structures in the solid phase, as well as the possibility of disordered phases.

PACS numbers: 71.10.Ca, 05.30.Fk, 75.10.-b, 75.10.Lp

Ever since the pioneering work of Wigner and Seitz [1] on the cohesive energy of metals, the calculation of the ground state energy of the interacting electron gas (quantum one component plasma, Fermi gas or simply jellium) became the object of considerable theoretical interest [2]. Indeed, the electron gas provides the simplest model in which non-trivial magnetic structures and electron localization can be realized by varying a single parameter, namely the average electron density ρ .

In the present paper we investigate the relative stability of various broken symmetry phases of the nonrelativistic three-dimensional electron gas, both fluid and solid, using stochastic methods. We report on a macroscopic instability of the Fermi gas which involves partial spin-polarization (weak ferromagnetism), in such a way that the paramagnetic to ferromagnetic (full spinpolarization) transition is not first order, as previously assumed, but a continuous one. Moreover we find that the transition to a Wigner crystal occurs at a significantly larger density than the value commonly accepted [3], and that near the quantum freezing transition the fcc and bcc crystal phases are nearly degenerate.

The jellium model consists of N electrons enclosed in a box of volume Ω (periodically repeated in space) in the presence of a neutralizing background of positive charge. Two parameters characterize its zero temperature phase diagram, namely the particle density $\rho = N/\Omega$ and the spin polarization $\zeta = |N_{\uparrow} - N_{\downarrow}|/N$, where $N_{\uparrow(\downarrow)}$ is the number of spin-up(down) electrons $(N = N_{\uparrow} + N_{\downarrow})$. The system is governed by the Hamiltonian (Hartree a.u.)

$$\widehat{H} = \sum_{i=1}^{N} \frac{\mathbf{p}_{i}^{2}}{2} + \sum_{i< j}^{N} \frac{1}{|\mathbf{r}_{i} - \mathbf{r}_{j}|} + \Lambda , \qquad (1)$$

where \mathbf{r}_i and \mathbf{p}_i) are the position and linear momentum of particle *i*, and Λ is a constant representing the effect of the background. Since we are interested in the macroscopic properties of this model system, the thermodynamic limit $(N, \Omega \to \infty)$, keeping ρ constant) is to be performed in the end by finite size extrapolation.

Elementary scaling arguments indicate that the kinetic energy term in (1) goes as $1/r_s^2$ (r_s is the Wigner-Seitz radius in units of the Bohr radius and its relation to the density is $\rho^{-1} = \frac{4\pi}{3}r_s^3$, while the potential energy scales as $1/r_s$. Depending on the relative strength between Coulomb and kinetic energies, we can characterize three different regimes: the weak $(r_s \leq 1)$, intermediate $(1 \leq r_s \leq 10)$, and strong $(r_s \geq 10)$ Coulomb coupling regimes. The random-phase approximation [2] provides an accurate description of the weak-coupling regime. The intermediate coupling region, of direct interest for density functional calculations, has been extensively studied by numerical [3,4] and semi-analytic methods [5]. Not surprisingly, the least known regime is the strongly correlated one, for which an early quantum Monte Carlo calculation [3] is still the most authoritative study.

To delve into the strong coupling regime we employ the variational (VMC) and diffusion (DMC) quantum Monte Carlo methods. The starting point is provided by a variational wave function of the Jastrow type:

$$\Psi_T(\mathcal{R}) = J[\mathcal{R}, \Sigma] \det_{\uparrow}[\varphi] \cdot \det_{\downarrow}[\varphi] , \ \Psi_T(\mathcal{R}) \in \mathbb{R}$$

where $\det_{\uparrow(\downarrow)}[\varphi]$ is a spin up(down) Slater determinant of one-electron orbitals φ that are either plane waves (fluid phases) or localized functions (crystal phases). In the equation above, $\mathcal{R} = (\mathbf{r}_1, \cdots, \mathbf{r}_N)$ and $\Sigma = (\sigma_1, \cdots, \sigma_N)$ represent the full set of positions and spins of the electrons in the system. Considering only 2-body correlations, the Jastrow factor can be written as: $J[\mathcal{R}, \Sigma] =$ $\prod_{i< j}^{N} \exp[v_{ij}(|\mathbf{r}_i - \mathbf{r}_j|)].$ For an infinite system the optimal $v_{ij}(r)$ should decay as 1/r at large distances to account for the correct plasmon dispersion relation. For large but finite systems, however, that is not the case and to reproduce the long distance behavior without resorting to expensive evaluations of v's by Ewald sums, we consider a finite range v_{ij} , vanishing outside a sphere of radius R_t tangential to the unit cell: $v_{ij}(r) = 0$ if $r > R_t$. We have verified that this truncation involves an insignificant loss of correlation energy at the variational

level [6]. Inside the sphere v_{ij} , which is different for like and unlike spin electrons, is given by:

$$v_{ij}(r) = \bar{v}_{ij}(r) + A_{ij} \exp[-\alpha_{ij}r^2]$$
, (2)

and

$$\bar{v}_{ij} = \begin{cases} \frac{a_{ij} r + b_{ij} r^2}{1 + c_{ij} r + d_{ij} r^2} + s_{ij} & , r < R_b \\ \sum_{k=0}^{5} f_k (r - R_b)^k & , r > R_b \end{cases}$$
(3)

The $\{a_{ij}\}\$ are determined by the electron-electron cusp condition [7], while $\{b_{ij}, c_{ij}, d_{ij}, s_{ij}, A_{ij}, \alpha_{ij}\}\$ and R_b are variational parameters. The $\{f_k\}\$ are chosen in such a way that Ψ_T and its two first derivatives are continuous everywhere. The one-electron orbitals used for the crystal phases are exponentials of a Padé function:

$$\varphi_{\mathbf{j}}(\mathbf{r}) = \exp\left[\frac{-k_1|\mathbf{r} - \mathbf{R}_{\mathbf{j}}|^2}{1 + k_2|\mathbf{r} - \mathbf{R}_{\mathbf{j}}|}\right],\tag{4}$$

where the (positive) constants k_1, k_2 are also variational parameters, and the fixed vectors $\{\mathbf{R_j}, \mathbf{j} = 1, N\}$ are distributed on a regular (bcc or fcc) lattice. This analytic form allows $\varphi_{\mathbf{j}}$ to change from Gaussian close to each $\mathbf{R_j}$ to a decaying exponential far from the localization centers. The fluid states are eigenstates of zero total momentum, while the solid ones are eigenstates of finite lattice translations with vanishing total crystal momentum. Both are eigenstates of the z-component of the total spin S_z with eigenvalue $\hbar M = \hbar (N_{\uparrow} - N_{\downarrow})/2$. All the free coefficients are optimized by the variance minimization technique introduced in Ref. [8]. The optimized wave functions are used to drive the DMC simulation [9].

Several features of the phase diagram discussed below depend upon the accurate evaluation of tiny energy differences. To provide a basis to estimate the reliability of our results, we report here the relevant aspects of our computation, including an estimate for the statistical and systematic errors. First of all, because of the high quality of the wave functions, and the relatively long runs, statistical errors are the least important source of uncertainties: for all r_s , the statistical error is less than 1 % of the correlation energy. Moreover, again because of the high variational freedom in the wave function, the energy gain in going from VMC to DMC is relatively small. As expected, the difference $\delta E = E_{tot}^{VMC} - E_{tot}^{DMC}$ is largest at low r_s [10], because the *n*-body contributions not included in our Jastrow function become more important at high density [11]. Moreover, for each r_s we find that $\delta E(\zeta)$ is larger for $\zeta = 0$ than for $\zeta = 1$, and, in between, the ζ dependence of δE is well represented by the simple interpolation: $\delta E(\zeta) = \delta E(0) + (\delta E(1) - \delta E(0)) \zeta^2$.

For the fluid phase the most important source of uncertainty in our calculations is the finite-size extrapolation to the thermodynamic limit. We applied the extrapolation scheme proposed in Ref. [3]:

$$E_{\infty}(\boldsymbol{\zeta}) = E_{N}(\boldsymbol{\zeta}) - \Delta t_{N}(\boldsymbol{\zeta}) + (N/b(\boldsymbol{\zeta}) - 1/\Delta v_{N}(\boldsymbol{\zeta}))^{-1} , \quad (5)$$

where $\boldsymbol{\zeta} = (r_s, \zeta), E_N(\boldsymbol{\zeta})$ is the total energy of the finite periodic system, b and E_{∞} are fitting parameters, Δt_N and Δv_N describe the size dependence of Hartree-Fock kinetic and exchange energies $(\Delta t_N = t_N^{HF} - t_\infty^{HF})$, $\Delta v_N = v_N^{HF} - v_\infty^{HF}$). The parameter E_∞ is the extrapolated value of the total energy per electron. Following Ref. [4] we assume $b(\boldsymbol{\zeta}) = b_0(r_s) + b_1(r_s) \boldsymbol{\zeta}^4$. The parameters $b_0(r_s)$ and $b_1(r_s)$ are obtained from the VMC total energies of an extended set of systems (N = 1062, 1450,and 1930 for $\zeta = 0, N = 531, 725, 965$ for $\zeta = 1$). This form is used to extrapolate all the energies computed by VMC and DMC for unpolarized, partially and fully polarized fluid systems. For lower densities the extrapolation is less critical but still important. We verified that for the crystal phases the finite size extrapolation error is comparable to the statistical one if N > 500. Therefore, the results for N = 686 (bcc) and N = 864 (fcc) are assumed to be equal to the $N \to \infty$ limit.

Extensive DMC calculations are performed for systems with N = 1062 (paramagnetic fluid), N = 725 (ferromagnetic fluid), N = 686 (ferro- and antiferro-magnetic bcc crystal), N = 864 (ferromagnetic fcc phase). For $r_s \leq 10$ our results agree, within the error bar, with those reported in Ref. [4]. Representative values for the correlation energy extrapolated to the thermodynamic limit are reported in Table I, and Fig. 1 shows a phase diagram displaying the stability range of the paramagnetic fluid, ferromagnetic fluid, and bcc (ferromagnetic) Wigner phases. It is apparent that a transition from the paramagnetic to a ferromagnetic fluid phase takes place around $r_s \approx 25$, while from the fluid to the crystal it is at $r_s \approx 65$. We found that the fcc is slightly less stable than the bcc structure, and more stable than the fluid phase at $r_s = 70$. The total energy difference between the two Wigner phases $(10^{-3} \text{ eV/electron})$ is five times smaller than the one between fluid and bcc crystal, and is, therefore, at the limit of our resolution.

The close competition of the fluid and different crystal forms for $r_s \approx 70$ suggests that a metastable amorphous phase could be formed in this region of the phase diagram, because the large number of available configurations, and the tiny energy differences could make the crystallization kinetics exceedingly slow. Preliminary calculations, in which the regular lattice of $\{\mathbf{R_j}\}$ vectors are displaced by random amounts (up to 25 % of the nearest neighbor distance), show that the total energy increases only very slowly with increasing disorder.

We now turn to the analysis of the spin dependence of the total energy near the ferromagnetic and freezing transitions. To ease the analysis, we perform a detailed

investigation at the VMC level, and then test the validity of the resulting picture by a few DMC calculations.

Regarding the magnetic phase transition, we compute the total energy for several sizes and partial spin polarizations [12] in the range $0.8 \le r_s \le 30$. The extrapolated results for $r_s = 25$ are reported in Fig. 2. It is clear that, at this density, the ground state has partial spin polarization (weak ferromagnet). The full set of data is used to fit an interpolation for the total energy (See Ref. [13]):

$$E_{tot}(\boldsymbol{\zeta}) = E_{tot}^{HF}(\boldsymbol{\zeta}) + \epsilon_0(r_s) + (\epsilon_1(r_s) - \epsilon_0(r_s)) \cdot (\Gamma_1(r_s) \ \boldsymbol{\zeta}^2 + \Gamma_2(r_s) \ \boldsymbol{\zeta}^4) , \quad (6)$$

where $E_{tot}^{HF}(\boldsymbol{\zeta})$ is the Hartree-Fock energy. In this expression $\epsilon_{0(1)}(r_s)$ is the correlation energy of the paramagnetic(fully polarized) fluid, and together with $\Gamma_1(r_s)$ and $\Gamma_2(r_s)$ are fitted to the functional form

$$\mathcal{G}(r_s) = -2A(1 + \alpha_1 r_s)$$
$$\ln\left[1 + \frac{1}{2A(\beta_1 r_s^{1/2} + \beta_2 r_s + \beta_3 r_s^{3/2} + \beta_4 r_s^2)}\right] , \quad (7)$$

whose motivation, and connection to the exact highdensity limit for $\epsilon_{0(1)}$ are discussed in Ref. [13]. This expression for the energy is minimized with respect to ζ at fixed r_s to identify the ground state spin polarization. The stable ζ as a function of r_s is shown in the inset of Fig. 2. It is manifest that the magnetic transition is a continuous one, in contrast to what is predicted on the basis of simpler interpolations, like the (widely used) form proposed by Perdew and Zunger [14].

We emphasize that the interpolation used to determine the ground state polarization is based on VMC calculations. Nevertheless, as mentioned above, the total energy difference between the VMC and DMC results is small, and has a smooth and predictable dependence on ζ . Adding $\delta E(\zeta)$ to the fitted total energies does not change the transition from continuous to discontinuous, although it moves it slightly towards higher values of r_s (e.g. $\zeta = 0.5$ polarization is stable at $r_s = 26$ in VMC, while it is at $r_s = 30$ in DMC). We also remind that our calculations rely on the fixed-node (FN) approximation, and, at present, we cannot exclude that releasing the nodal constraints could change the nature of the magnetic transition. However, recent computations reported in Ref. [11] show that the FN error decreases rapidly with decreasing density, and is small already at $r_s = 20$.

Additional evidence supporting the picture of a magnetic instability and a continuous phase transition is provided by the analysis of the radial distribution function and structure factor, displaying for $r_s \approx 30$ long range spin-spin correlations even for nominally unpolarized systems ($N_{\uparrow} = N_{\downarrow}$.) This is illustrated in Fig. 3, where the spin-spin radial distribution function $(g_{SS}(r) = 2[g_{\uparrow\uparrow}(r) - g_{\uparrow\downarrow}(r)])$ is plotted for two densities close to the instability [15]. At $r_s = 20$, g_{SS} displays the expected depletion hole for parallel spins, reflecting the preference of the system for spin alternation at short distances. At $r_s = 25$, instead, the spin correlation is small and positive at short range, and oscillating at long range, pointing to the formation of magnetic domains with partial spin polarization. This interpretation in terms of domains is confirmed by careful analysis of snapshot configurations.

Indirect support to our findings comes also from recent experiments performed in doped hexaborides $(Ca_{1-x}La_xB_6)$ [16]. These authors report a weak ferromagnetic phase at low carrier concentration $(r_s = 28)$ with an ordered moment corresponding to a partial spin polarization of about 10 %. Moreover, the observed Curie temperature, which is as high as 600 K, is of the same order of magnitude as the Fermi energy indicating that this represents the natural energy scale of the spin system.

The magnetic phase diagram near the Wigner phase transition is somewhat simpler. For $70 \leq r_s \leq 100$ the exchange energy, although small in absolute terms, is still one order of magnitude larger than the correlation energy, and therefore it is not surprising that the ferromagnetic bcc structure is more stable than the antiferromagnetic spin ordering. However, both at the VMC and DMC level, the energy difference between these two states is very small (~ 1 % of the correlation energy), and only the systematic trend $E_{tot}^{ferro} < E_{tot}^{antiferro}$ for $70 \leq r_s \leq 100$ gives us some confidence in this result. As pointed out in the case of the translational disorder, because of entropy and kinetics the spin glass phase could be the most relevant one for low density electron systems.

In conclusion, using stochastic methods we have studied the magnetic and freezing quantum transitions of the fermionic one component plasma. We find that, contrary to the commonly accepted picture, the paramagnetic to the ferromagnetic fluid transition is a continuous one, occurring over the $25 \leq r_s \leq 35$ density range, which has been approached in experiments by doping highly correlated solids [16]. The transition to the bcc Wigner crystal is first order, it occurs at $r_s = 65 \pm 10$ and joins two fully polarized spin states. Where available, our results for the transition densities disagree substantially from those of a previous study [3]. We think that the disagreement is due to the extrapolation of the finite size results to the thermodynamics limit. In our case, the importance of this extrapolation has been limited by performing computations for systems with up to 2000 electrons, in this way reducing the corresponding uncertainties. Finally, we recall that our analysis is based on a selected set of broken symmetry states. There exists the possibility of other instabilities such as the inhomogeneous spin-density-wave state or superconducting states which we have not considered in the present calculation.

G.O. acknowledges support from an Oppenheimer fellowship and thanks the Aspen Center for Physics for

its hospitality. We are thankful to E. Abrahams, G. Bachelet, Z. Fisk, M. Jones, R. O. Jones, K. Sturm and S. Trugman for illuminating discussions.

- [15] For consistency with Fig. 2, we report in Fig. 3 the results of the VMC calculation. A similar picture is obtained by DMC at a slightly lower density.
- [16] D.P. Young *et al*, submitted to Nature.
- 1 102050100 $\zeta = 0$ 1.5310.4970.313 0.15311.530.5121.620.5050.3130.1550.0868 0.814 0.0968 0.0549 $\zeta = 1$ 0.2830.18370.7940.2810.0965 0.0564 0.860.2860.1950

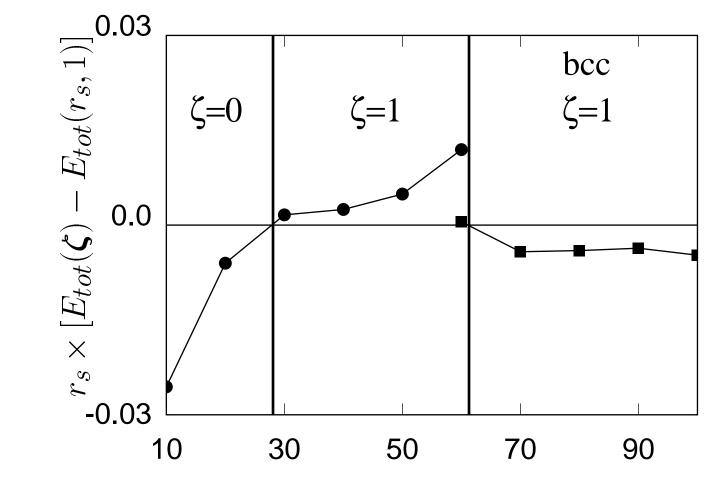
TABLE I. Minus the DMC correlation energies (in eV) extrapolated to the thermodynamic limit. For each ζ , the first row refers to the present results, while the second and third rows correspond to Ref. [4] and Ref. [3], respectively. The statistical error affects the last decimal digit.

FIG. 1. Total energy difference (eV) times r_s of: (•) the paramagnetic and the ferromagnetic fluids; (\blacksquare) the ferromagnetic bcc crystal and the ferromagnetic fluid. The statistical error bar is comparable to the size of the symbols. The ferromagnetic fluid is stable when both symbols are above zero.

FIG. 2. Total energy (VMC) as a function of ζ for a weak ferromagnetic state. The statistical error bar is reported for the lowest energy point. The inset shows the equilibrium spin polarization r_s as a function of ζ . For $\zeta \sim 0$ and $\zeta \sim 1$ the results depend significantly on the interpolation (see text), and therefore they have not been reported in the figure.

FIG. 3. Spin-spin correlation function (VMC) near the magnetic instability.

- [1] E.P. Wigner and F. Seitz, Phys. Rev. 43, 804 (1933).
- [2] D. Pines and P. Nozières, The Theory of Quantum Liquids (Addison-Wesley, New York, 1989), Vol I.
- [3] D.M. Ceperley and B.J. Alder, Phys. Rev. Lett. 45, 566 (1980).
- [4] G. Ortiz and P. Ballone, Phys. Rev. B. 50, 1391 (1994); ibid 56, 9970 (1997).
- [5] K.S. Singwi, M.P. Tosi, R.H. Land and A. Sjölander, Phys. Rev. **176**, 589 (1968).
- [6] At the DMC level this approximation is irrelevant because those "bosonic" correlations are fully recovered in the diffusion process; only the variance of averages measured in the simulation is affected.
- [7] T. Kato, Comm. Pure Appl. Math. 10, 151 (1957).
- [8] C. Umrigar, J. Wilkins, and K. Wilson, Phys. Rev. Lett. 60, 1719 (1988).
- [9] P.J. Reynolds, D.M. Ceperley, B.J. Alder, and W.A. Lester, Jr., J. Chem. Phys. 77, 5593 (1982); C.J. Umrigar, M.P. Nightingale, and K.J. Runge, J. Chem. Phys. 99, 2865 (1993).
- [10] We find δE is 0.027 eV at $r_s = 1$, and 0.0059 eV at $r_s = 10$ with $\zeta = 0$.
- [11] Y. Kwon, D.M. Ceperley, and R.M. Martin, Phys. Rev. B xxx (1998).
- [12] N = 1256, $\zeta = 0.154$; N = 1136, $\zeta = 0.276$; N = 1056, $\zeta = 0.373$, N = 954, $\zeta = 0.520$, N = 838, $\zeta = 0.730$.
- [13] J.P. Perdew and Y. Wang, Phys. Rev. B 45, 13244 (1992).
- [14] J.P. Perdew and A. Zunger, Phys. Rev. B 23, 5048 (1981).



 r_s

